Brief Definitive Report

N-formylpeptides Induce Two Distinct Concentration Optima for Mouse Neutrophil Chemotaxis by Differential Interaction with Two *N*-formylpeptide Receptor (FPR) Subtypes: Molecular Characterization of FPR2, a Second Mouse Neutrophil FPR

By Jennifer K. Hartt, Grant Barish, Philip M. Murphy, and Ji-Liang Gao

From the Laboratory of Host Defenses, National Institute of Allergy and Infectious Diseases, National Institutes of Health, Bethesda, Maryland 20892

Summary

The *N*-formylpeptide receptor (FPR) is a G protein–coupled receptor that mediates mammalian phagocyte chemotactic responses to bacterial *N*-formylpeptides. Here we show that a mouse gene named *Fpr-rs2* encodes a second *N*-formylpeptide receptor subtype selective for neutrophils which we have provisionally named FPR2. The prototype *N*-formylpeptide fMLF induced calcium flux and chemotaxis in human embryonic kidney (HEK) 293 cells stably transfected with FPR2. The EC_{50}s, ~5 μM for calcium flux and chemotaxis, were ~100-fold greater than the corresponding values for mouse FPR-transfected HEK 293 cells. Consistent with this, fMLF induced two distinct concentration optima for chemotaxis of normal mouse neutrophils, but only the high concentration optimum for chemotaxis of neutrophils from FPR knockout mice. Based on these data, we hypothesize that high- and low-affinity *N*-formylpeptide receptors, FPR and FPR2, respectively, may function in vivo as a relay mediating neutrophil migration through the high and low concentration portions of *N*-formylpeptide gradients.

Key words: chemoattractant • inflammation • neutrophil • G protein–coupled receptor • phagocyte

The *N*-formylpeptides are cleavage products of bacterial and mitochondrial proteins, and serve as powerful chemoattractants for mammalian phagocytes (1–3). Based on their chemotactic actions, it has been hypothesized that *N*-formylpeptides attract phagocytes to sites of infection and therefore play an important role in antibacterial host defense (4). Like other chemoattractants, they act through seven-transmembrane-domain G protein–coupled receptors (5).

Two functional *N*-formylpeptide receptors, designated FPR and FPRL1R, and one related putative receptor, designated FPRL2, have been identified by human gene cloning (6–11). FPR and FPRL1R bind the prototypical *N*-formylpeptide fMet-Leu-Phe (fMLF) with high and low affinity, respectively. The K_d for FPR is ~3 nM, whereas that for FPRL1R is >100 times higher (10, 12). fMLF has been reported to induce calcium mobilization in cells transfected with FPR or FPRL1R and chemotaxis in cells transfected with FPR, but does not induce chemotaxis in cells transfected with FPRL1R when tested at concentrations as high as 2 μM (8, 10, 13, 14). FPRL1R has also been reported to bind lipoxin A_4, a lipid derivative of arachidonate metabolism, with high affinity. Functions of lipoxin A_4 mediated by FPRL1R include induction of GTPase activity and production of arachidonic acid; however, it has not been shown to induce calcium flux or chemotaxis (15). To our knowledge, FPRL1R is the only receptor whose agonists include both a peptide and a lipid. Recently, the range of potential biological actions of FPRL1R has become further complicated by the discovery that serum amyloid A (SAA), an acute phase reactant in inflammation, and T21, an ectodomain peptide of HIV-1 gp41, are also functional ligands for FPRL1R (16, 17). A second gp41 peptide named T20, which is a powerful blocker of HIV-1 entry currently in clinical trials, has been reported to be a functional ligand for FPR (18, 19).

To identify biological roles for these molecules, we have been studying their mouse counterparts. We previously characterized mouse FPR and have developed mice lacking this receptor by targeted gene deletion (20, 21). $FPR^{-/-}$ mice revealed an important role for FPR in innate host defense against *Listeria monocytogenes* (21). We have also

cloned five related mouse genes, designated *Fpr-rs1*, *Fpr-rs2*, *Fpr-rs3*, *Fpr-rs4*, and *Fpr-rs5* (22). Extensive cross-hybridization analysis failed to find more than three related human genes, indicating that the FPR gene cluster has undergone differential lineage-specific expansion in mammals. This has created problems in defining orthologous relationships, particularly in defining the mouse FPRL1 orthologue. *Fpr-rs1* and *Fpr-rs2* are most similar to human FPRL1 (both show ~75% nucleotide identity in the open reading frame [ORF]), whereas the other three genes form a separate cluster with slightly lower sequence relatedness to FPRL1 (22). Like FPRL1, both *Fpr-rs1* and *Fpr-rs2* are expressed in leukocytes, although expression in specific leukocyte subsets has not previously been defined.

Chinese hamster ovary (CHO) cells transfected with *Fpr-rs1* have been demonstrated to bind lipoxin A_4, and the encoded receptor has therefore been named LXA_4R (23). This suggested that *Fpr-rs1* is the orthologue of FPRL1 but raised unanswered questions about its specificity for *N*-formylpeptides and about the ligand specificity of *Fpr-rs2*, as well as about the functional relationship of these molecules to FPR. Here we show that *Fpr-rs2* encodes a second mouse neutrophil fMLF receptor subtype, which we now provisionally name FPR2, which operates at higher concentrations of ligand than FPR.

Materials and Methods

Mouse Leukocyte Purification. Development of FPR knockout mice has been described previously (21). Mice used in this study were from $FPR^{+/-} \times FPR^{+/-}$ matings of an F1 backcross of $FPR^{+/-}$ 129/Sv with wild-type C57Bl/6 mice. Leukocytes were harvested from the peritoneal cavity of $FPR^{+/+}$ and $FPR^{-/-}$ mice after thioglycollate (TG) irritation, as described previously (21). Cells obtained after 3 h were >90% neutrophils, whereas cells obtained after 72 h were >90% macrophages, as determined by the morphologic appearance of Diff-Quick-stained preparations.

RNA Analysis. Cells were lysed, and total RNA was prepared using the RNA STAT-60 protocol (Tel-Test, Inc.). RNA (10 μg) was separated on a denaturing agarose gel, and Northern blots were prepared by standard methods (24). Blots were hybridized with a full-length *Fpr-rs2* ORF probe, which was labeled with ^{32}P-dCTP using a random-primer DNA labeling kit (Boehringer Mannheim). To control for RNA loading, the blots were also probed separately with a 49-bp oligonucleotide from the 5′ terminal end of the actin gene, which was labeled with a DNA 5′ end labeling kit (Boehringer Mannheim).

Creation of a Cell Line Expressing FPR2. The *Fpr-rs2* ORF was amplified from genomic clone 7 (22) using the upper strand primer 5′-ATATAAGCTTGCCACC*ATG*GATTATAAAGATGATGATAAA*GAATTC*GAATCCAACTACTCCATCCATCTGAATG-3′, which contains a Flag epitope tag (underlined), an EcoRI site (italicized), and an ATG initiating codon (bold); and lower strand primer 5′-CG*CTCGAG***TCA**TGGGGCCTTTAACTCAATGTCTG-3′, which contains an XhoI site (italicized sequence) and the termination codon (bold). The 1.1-kb PCR fragment was then ligated into pCR2.1. Sequence fidelity was verified, and the correct insert was then subcloned between the NotI and XhoI sites of pcDNA3 (Invitrogen). Human embryonic kidney (HEK) 293 cells were maintained in DMEM with 10% FBS. 10^7 cells in log phase were electroporated with 20 μg of plasmid DNA using a GenePulser (Bio-Rad Laboratories). Cell colonies resistant to 2 g/liter G-418 (GIBCO BRL) were isolated and expanded in DMEM with 10% FBS and 2 g/liter G-418.

Intracellular [Ca^{2+}] Measurements. Cells (~10^7/ml) were incubated in HBSS and 2.5 μM Fura-2 AM (Molecular Probes, Inc.) for 30–60 min at 37°C in the dark. The cells were then washed with HBSS and resuspended at 10^7 cells/ml. 4×10^6 cells were stimulated in a total volume of 2 ml in a continuously stirred cuvette at 37°C in a fluorimeter (Photon Technology, Inc.). fMLF, MLF, and recombinant C5a were obtained from Sigma Chemical Co. The chemokines IL-8, macrophage-inflammatory protein (MIP)-1β, and monocyte-chemotactic protein (MCP)-3 were obtained from Peprotech. The data were recorded every 200 ms as the relative ratio of fluorescence emitted at 510 nm after sequential excitation at 340 and 380 nm. For some experiments, cells were incubated with 250 ng/ml pertussis toxin for 4 h before functional assay.

Chemotaxis. HEK 293 cells were detached from flasks by replacing media with 0.05% trypsin (Quality Biological) and incubating at room temperature for ~1 min. DMEM containing 20% FBS was added, and the cells were harvested, pelleted, and resuspended at 10^6 cells/ml in RPMI 1640 supplemented with 1% BSA and 20 mM Hepes. fMLF was loaded at varying concentrations in the lower compartment of a 48-well microchemotaxis chamber (NeuroProbe). To distinguish chemotaxis from chemokinesis, additional experiments were carried out in which an equal concentration of fMLF was tested simultaneously in the upper and lower compartments. The chamber was soaked in 1% SDS overnight and washed before each experiment. A polyvinylpyrrolidone-free polycarbonate filter (10- and 3-μm pores for HEK 293 cells and neutrophils, respectively) was used. For experiments with HEK 293 cells, the filters were coated with 0.05 mg/ml rat tail collagen in RPMI 1640 and 70 mM Hepes for 2 h and dried before each experiment. The filter, coated side down, was placed between the upper and lower compartments of the chamber, and 50 μl of 10^6 HEK 293 cells/ml was loaded in the upper compartment. The chemotaxis chamber was incubated at 37°C, 100% humidity, and 5% CO_2 for 5 h for HEK 293 cells and 45 min for neutrophils. The filter was then removed, washed, fixed, and stained. Cells that migrated through the filter were counted microscopically under high power. All conditions were tested in triplicate.

Results

Fpr-rs2 Is Expressed in Mouse Phagocytes. Previously, we reported that *Fpr-rs2* is expressed in unfractionated peripheral blood leukocytes (22). To determine the expression pattern in finer detail, we used Northern blot hybridization to probe total RNA from peritoneal cells elicited 3 and 72 h after instillation of TG. The elicited peritoneal cell populations were markedly enriched in neutrophils and macrophages at 3 and 72 h, respectively (>90% pure). The residual 10% of cells were mainly mononuclear cells and neutrophils in the 3- and 72-h cell populations, respectively. Specific mRNA bands were detected in both the 3- and 72-h TG-elicited peritoneal cells. In both cases, two classes of transcripts

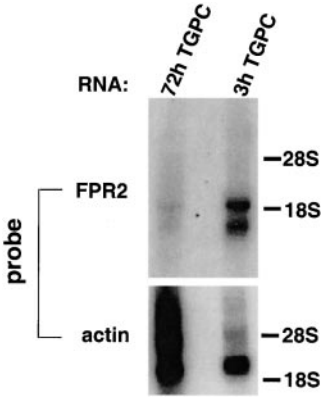

Figure 1. Distribution of FPR2 mRNA in mouse leukocytes. A Northern blot containing total RNA from peritoneal cells elicited 3 and 72 h after instillation of TG (3h TGPC and 72h TGPC) was serially hybridized to a ^{32}P-labeled *Fpr-rs2* ORF probe encoding FPR2 and a ^{32}P-labeled actin probe, both under high stringency conditions. 3- and 72-h TG-elicited peritoneal cells were enriched in neutrophils and macrophages, respectively (>90%). After hybridization with *Fpr-rs2* and actin, the blot was exposed for 3 and 2 d, respectively, to x-ray film. The positions of 18S and 28S ribosomal bands are indicated at the right. The 72h TGPC lane was deliberately overloaded with RNA, as indicated by the actin hybridization, to test for low abundance mRNA.

(~1.5 and 1.9 kb) were observed, and the signal strength was similar for each class within each sample. However, signals from the 3-h cells were much stronger than from the 72-h cells (Fig. 1). Note that 72-h RNA was deliberately overloaded relative to 3-h RNA, as revealed by hybridization with an actin probe. A reasonable interpretation of these results, consistent with the functional data that follows, is that *Fpr-rs2* is primarily expressed in neutrophils, and the weak signal in the 72-h cells is due to neutrophils, which make up a small minority of the total cell population. An alternative explanation is that monocytes express *Fpr-rs2* in the circulation, but not after extravasation.

Fpr-rs2 Encodes a Low-affinity G Protein–coupled FPR. To assess whether *Fpr-rs2* encodes a functional FPR, we performed a gain-of-function genetic test by measuring fMLF-induced intracellular Ca^{2+} flux in HEK 293 cell lines stably transfected with expression plasmids containing the *Fpr-rs1* or *Fpr-rs2* ORFs.

In the initial screen, we tested 16 G-418–resistant HEK 293 cell colonies derived from the same transfection, all of which responded to 10 μM fMLF. In contrast, nonformylated MLF at 1 μM, C5a at 10 nM, and the chemokines IL-8, MIP-1β, and MCP-3 at 100 nM or greater did not induce a response. Also, *Fpr-rs1*–transfected cells, maintained in the same selective conditions, consistently failed to respond to fMLF at concentrations as high as 100 μM (Fig. 2 A). Higher concentrations could not be tested for technical reasons due to the hydrophobicity of fMLF. Based on this result, we infer that *Fpr-rs2* encodes an FPR, which we provisionally name FPR2.

Four cell lines that gave particularly strong responses, designated L4-7, L4-14, L4-15, and L4-16, were selected for further study. In each case, the calcium flux responses were concentration dependent and saturable, with an EC_{50} of 5.3 ± 0.3 μM (n = 5, each cell line tested at least once; Fig. 2 C). HEK 293 cells transfected with mouse FPR also exhibited a calcium flux response to fMLF that was concentration dependent and saturable; however, the EC_{50}, ~50 nM, was much lower than for FPR2 (Fig. 2 C). This value is consistent with that previously reported for expression of mouse FPR in frog oocytes in a calcium-release assay (20).

When FPR2-transfected cells were sequentially stimu-

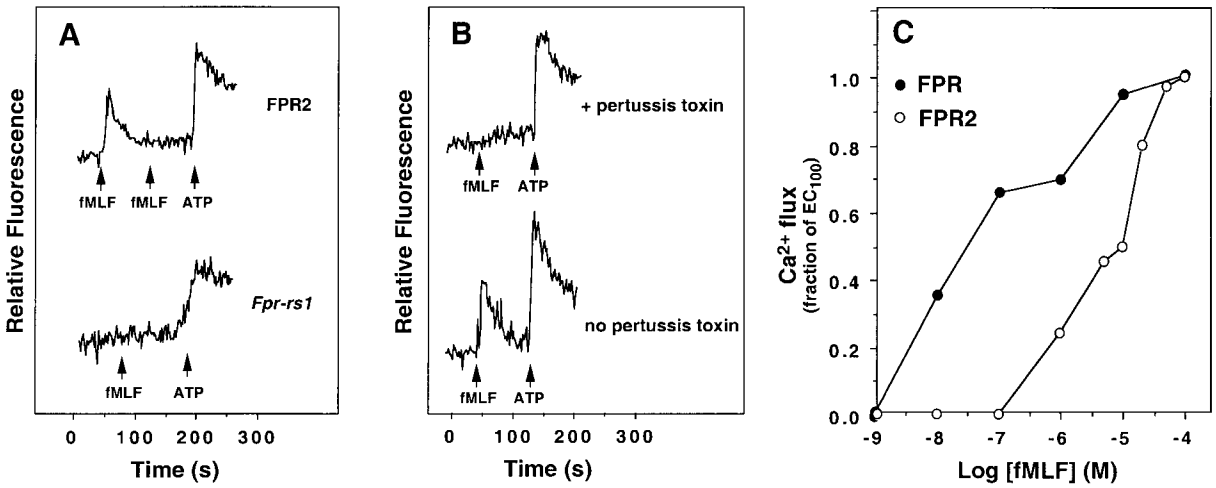

Figure 2. Mouse FPR2 is a G protein–coupled receptor specific for fMLF. Receptor activation was monitored in real time by calcium flux assay. (A) fMLF specificity. *Fpr-rs1*– and FPR2-transfected HEK 293 cells were stimulated with 100 μM fMLF at the times indicated by arrows. Responses are in relative fluorescence units. Results shown for FPR2 are for clone L4-16 and are representative of >5 experiments with this clone and 1 experiment with 15 other FPR2-specific clones. 10 μM ATP, which activates an endogenous ATP signaling pathway, was used as a positive control. (B) Pertussis toxin blockade of FPR2 signaling. FPR2-transfected cells cultured in the presence and absence of 250 ng/ml pertussis toxin were stimulated with 100 μM fMLF. As a positive control, toxin-treated cells were also stimulated with 10 μM ATP, which induces pertussis toxin–resistant calcium flux. The results are representative of four independent experiments. (C) Concentration dependence. Data for each curve are from separate experiments representative of at least five experiments each for the FPR2 cell line L4-16 and the FPR cell line mFPR-23. Data are derived from the peak amplitude of the calcium transient at each concentration tested, and are plotted as a fraction of the EC_{100}.

lated with 100 μM fMLF, no response was observed after the second stimulation, suggesting complete receptor desensitization by the first stimulus (Fig. 2 A). The fMLF response could also be abolished by pretreatment of FPR2-expressing cells with pertussis toxin, suggesting that the receptor is coupled to a G_i-type G protein (Fig. 2 B). As a control of cell integrity, we stimulated toxin-treated cells with 10 μM ATP, which induced a calcium flux at levels equivalent to the untreated cells.

To test the mechanism of fMLF induction of calcium flux in FPR2-transfected cells, we carried out radioligand binding assays using a ^{3}H-fMLF probe. Although human and mouse FPR-expressing cells exhibited specific binding, cells expressing FPR2 did not (data not shown). This is not surprising, since the highest concentration of ^{3}H-fMLF that could be meaningfully tested was 640 nM, which is below the threshold of detection of calcium flux induced by fMLF in FPR2-transfected cells. In contrast, the threshold for induction of calcium flux by fMLF in human and mouse FPR-transfected cells is ~0.5 and 10 nM, respectively. We conclude that FPR2 is most likely a low-affinity FPR.

FPR2 Is a Chemotactic Receptor. Given the reactivity of FPR2 to fMLF observed in the calcium flux assay, we next tested its ability to mediate chemotaxis. FPR2-expressing cells migrated in a concentration-dependent manner in response to fMLF with a threshold of ~1 μM. The EC_{50} was ~5 μM. In all experiments, the upward phase of the concentration–response curve was consistently superimposable with that of the calcium flux assay for the same FPR2-expressing cell line. Mouse FPR-expressing HEK 293 cell migration followed a clear-cut bell-shaped concentration–response curve whose EC_{50} was shifted ~10–100-fold to the left relative to the FPR2 curve (Fig. 3). The activity was specific for both receptors, since HEK 293 cells transfected with the related gene *Fpr-rs1* and selected with G-418 did not exhibit concentration-dependent migration in response to fMLF when tested with concentrations ranging from 0.1 nM to 100 μM (Fig. 3 B). To distinguish chemotaxis from chemokinesis, equal concentrations of fMLF were added to the upper and lower chambers of the chemotaxis apparatus. In this configuration, no dose-dependent cell migration was observed (Fig. 3 A). Therefore, FPR2 can not only cause intracellular signaling, but can also use those signals to elicit a chemotactic action by the cell.

FPR2 May Mediate Mouse Neutrophil Calcium Flux and Chemotaxis. To determine whether FPR2 may operate as a second mouse neutrophil fMLF receptor in primary cells, we examined fMLF responses by cells from FPR knockout mice. Previously, we reported that neutrophils from these mice failed to respond to fMLF either in calcium flux or chemotaxis assays at concentrations as high as 1 μM, and noted that this correlated well with the concentration–response relationship for HEK 293 cells expressing mouse FPR in the calcium flux assay (21).

However, having now discovered that the threshold for calcium flux in FPR2-expressing cells was ~1 μM, we retested neutrophils from these animals at higher concentrations and observed a concentration–response relationship that was virtually identical for $FPR^{-/-}$ neutrophils versus HEK 293 cells expressing FPR2 for both calcium flux and chemotaxis (Figs. 2–4). The EC_{50} value in $FPR^{-/-}$ neutrophils was ~6 μM for calcium flux, in close agreement with the value of 5.3 μM cited above for FPR2-expressing HEK 293 cells (compare Figs. 2 C and 4 A). The chemotaxis concentration–response curves were also very similar (compare Figs. 3 B and 4 B).

Calcium flux and chemotaxis experiments were also performed on neutrophils from wild-type mice using an expanded concentration range relative to what was used in our previous report, 1 nM to 100 μM (Fig. 4). In the calcium flux assay, the response saturated at 1 μM fMLF, which corresponds to the saturation concentration for

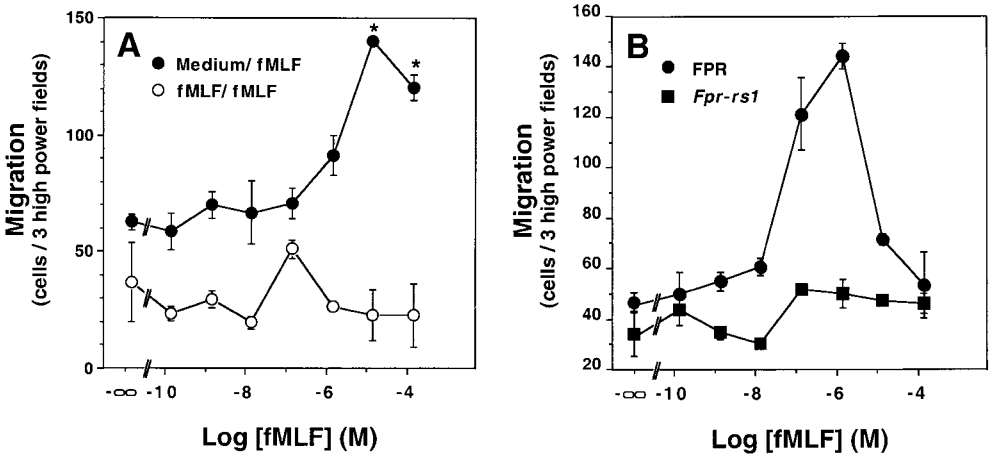

Figure 3. FPR2 is a chemotactic receptor. HEK 293 cells stably transfected with mouse FPR, FPR2, or *Fpr-rs1* were incubated in a microchemotaxis chamber for 5 h, and the number of migrating cells was counted. Data shown are from a single experiment representative of more than five separate experiments in each panel with a consistent pattern. (A) FPR2 transfectants with equal concentration of fMLF in the upper and lower chambers (fMLF/fMLF, open circles), or with fMLF in only the lower chamber (Medium/fMLF, filled circles). *Statistically significant difference between the points shown and baseline migration in the absence of fMLF, $P < 0.0005$ by Student's t test. (B) FPR transfectants (circles) and *Fpr-rs1* transfectants (squares).

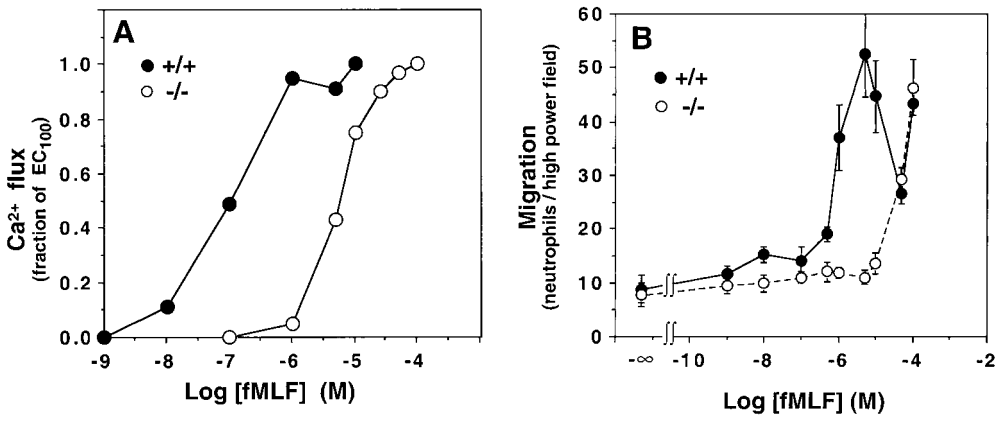

Figure 4. Mouse neutrophils lacking FPR respond to fMLF with a concentration dependence matching that of FPR2. Peritoneal leukocytes elicited by a 3-h challenge with TG (>90% neutrophils) from wild-type mice (+/+, filled symbols) and FPR knockout littermates (−/−, open symbols) were stimulated with the indicated concentration of fMLF. (A) Calcium flux. Data are derived from the peak amplitude of the calcium transient at each concentration tested, and are plotted as a fraction of the EC_{100}. Data are representative of more than five experiments. (B) Chemotaxis. Conditions were tested in triplicate. Each curve represents data from a single mouse of the given genotype. Data are representative of three experiments.

mouse FPR and the threshold concentration for FPR2 (Fig. 2 C). For chemotaxis, we observed an unusual, multiphasic concentration–response relationship, which was equivalent to the sum of the individual relationships for mouse FPR and FPR2 tested separately in HEK 293 cells (Fig. 3). A first peak was clearly resolved and consistently observed between 0.5 and 50 μM, and had an optimum of 5 μM. The curve then passed through a minimum at 50 μM, and then consistently increased at 100 μM. The second peak could not be fully resolved due to artifacts induced by DMSO required to solubilize fMLF at higher concentrations. However, its existence is strongly corroborated by a dose-dependent increase in migration of neutrophils from the $FPR^{-/-}$ mice over the same concentration range.

Discussion

In this study, we have identified dual concentration–response optima for normal mouse neutrophils in chemotaxis induced by the proinflammatory chemoattractant fMLF. For leukocytes, chemoattractant concentration–response relationships are classically described by a bell-shaped curve with a single optimum; the presence of a second optimum as we have described is highly unusual. The functional characteristics of FPR versus FPR2, the second mouse neutrophil low-affinity fMLF receptor subtype that we have identified, in conjunction with analysis of neutrophils from mice lacking the high-affinity fMLF receptor FPR, strongly suggest a molecular explanation for this anomaly in which FPR and FPR2 account for the low and high concentration–response optima, respectively.

The significance of this result relates to the dilemma of how leukocytes navigate through the highest portions of chemoattractant concentration gradients in which their high-affinity chemoattractant receptors are likely to become deactivated through receptor phosphorylation and/or sequestration mechanisms (25, 26). Our data suggest the hypothesis that distinct high- and low-affinity receptors for the same chemoattractant may work as a relay to sensitize the cell throughout the gradient, allowing it to arrive at the focus of inflammation.

Most work on leukocyte chemotactic receptors has focused on the identification of receptors that bind ligand in the low nanomolar range, so-called "high-affinity receptors," because binding is easy to measure with available radioligand probes. However, potentially important low-affinity ligand–receptor interactions have also been identified, such as multiple CXC chemokines for CXCR1 (27) and MIP-1β and MCP-1 for CCR1 (28). In this regard, the CXC chemokine neutrophil-activating peptide 2 (NAP-2) is particularly interesting since, like fMLF in our study, it appears to activate neutrophil chemotaxis via two concentration–response optima by high-affinity binding to CXCR2 and low-affinity binding to CXCR1 (29).

Alternative mechanisms of navigation may also exist, such as usage of high-affinity receptors at different points during the migration path through differential spatial expression of cognate chemoattractants, or by receptor recycling, or by a combination of these mechanisms. In this regard, chemokines may be particularly important for fine-tuning leukocyte migration to inflammatory sites.

In humans, the two functional FPRs, FPR and FPRL1R, also have high and low affinity, respectively, for fMLF (7, 10, 12). Consistent with this, in calcium flux assays, fMLF is ~100-fold more potent at FPR versus FPRL1R in vitro. This hierarchy is analogous to that for mouse FPR and FPR2. However, one significant difference is that, to date, FPRL1R has not been reported to be a chemotactic receptor, and its biological function remains unknown. Therefore, the discovery of FPR2 represents the first time that two chemotactic FPRs have been observed in a single species.

FPRL1R also binds lipoxin A_4 with high affinity (15), to our knowledge the only example of a receptor with both peptide and lipid ligands. In mice, the related gene *Fpr-rs1* encodes a receptor, LXA_4R, that binds lipoxin A_4 (23). Therefore, it would

appear that differential expansion of an ancestral FPR gene occurred during evolution between humans and mice, resulting in two mouse receptors that split the functions of human FPRL1R: FPR2 mediates responses to *N*-formylpeptides, whereas LXA_4R mediates responses to lipoxin A_4. This theory will need to be tested by additional experiments addressing the specificity of FPR2 for lipoxin A_4 and LXA_4R for fMLF. In addition, these receptors will need to be tested for their specificity for SAA and HIV-1 T21, which act at human FPRL1R, and HIV-1 T20, which acts at FPR (16–18). Moreover, alternative *N*-formylpeptides besides fMLF must be considered as potential physiological ligands for both FPR and FPR2.

In conclusion, since FPR and FPR2 are both expressed in neutrophils and are differentially sensitive to fMLF, we propose that they may act sequentially during the inflammatory response: FPR recruits neutrophils in the low concentration portion of an *N*-formylpeptide gradient, whereas FPR2 operates closer to the inflammatory focus where concentrations are expected to be highest and FPR is more likely to be desensitized. We are currently developing an FPR2 knockout mouse to test this hypothesis further, as well as to test the physiological role of FPR2 and its relationship to human chemoattractant signaling.

Address correspondence to Ji-Liang Gao, Laboratory of Host Defenses, NIAID, Bldg. 10, Rm. 11N113, National Institutes of Health, Bethesda, MD 20892. Phone: 301-496-2877; Fax: 301-402-4369; E-mail: jgao@nih.gov

G. Barish's present address is University of Michigan School of Medicine, Ann Arbor, MI 48105.

J.K. Hartt's present address is Immunology Department, Harvard Medical School, 200 Longwood Ave., Bldg. D-2, Rm. 137, Boston, MA 02115.

Submitted: 29 March 1999 Revised: 25 June 1999 Accepted: 6 July 1999

References

1. Schiffmann, E., B.A. Corcoran, and S.M. Wahl. 1975. *N*-formylmethionyl peptides as chemoattractants for leukocytes. *Proc. Natl. Acad. Sci. USA*. 72:1059–1063.
2. Marasco, W.A., S.H. Phan, H. Krutzsch, H.J. Showell, D.C. Feltner, R. Nairn, E.L. Becker, and P.A.Ward. 1984. Purification and identification of formyl-methionyl-leucyl-phenylalanine as the major peptide neutrophil chemotactic factor produced by *Escherichia coli*. *J. Biol. Chem*. 259:5430–5439.
3. Carp, H. 1982. Mitochondrial *N*-formylmethionyl proteins as chemoattractants for neutrophils. *J. Exp. Med*. 155:264–275.
4. Murphy, P.M. 1996. The N-formylpeptide chemotactic receptor. *In* Chemoattractant Ligands and Their Receptors. R. Horuk, editor. CRC Press, Inc., Boca Raton, FL. 269–299.
5. Murphy, P.M. 1994. The molecular biology of leukocyte chemoattractant receptors. *Annu. Rev. Immunol*. 12:593–633.
6. Boulay, F., M. Tardif, L. Brouchon, and P. Vignais. 1990. Synthesis and use of a novel N-formyl peptide derivative to isolate a human N-formyl peptide receptor cDNA. *Biochem. Biophys. Res. Commun*. 168:1103–1109.
7. Boulay, F., M. Tardif, L. Brouchon, and P. Vignais. 1990. The human N-formylpeptide receptor. Characterization of two cDNA isolates and evidence for a new subfamily of G-protein-coupled receptors. *Biochemistry*. 29:11123–11133.
8. Murphy, P.M., and D. McDermott. 1991. Functional expression of the human formyl peptide receptor in *Xenopus* oocytes requires a complementary human factor. *J. Biol. Chem*. 266:12560–12567.
9. Murphy, P.M., T. Ozcelik, R.T. Kenney, H.L. Tiffany, D. McDermott, and U. Francke. 1992. A structural homologue of the N-formyl peptide receptor. Characterization and chromosome mapping of a peptide chemoattractant receptor family. *J. Biol. Chem*. 267:7637–7643.
10. Ye, R.D., S.L. Cavanagh, O. Quehenberger, E.R. Prossnitz, and C.G. Cochrane. 1992. Isolation of a cDNA that encodes a novel granulocyte N-formyl peptide receptor. *Biochem. Biophys. Res. Commun*. 184:582–589.
11. Bao, L., N.P. Gerard, R.L. Eddy, Jr., T.B. Shows, and C. Gerard. 1992. Mapping of genes for the human C5a receptor (C5AR), human FMLP receptor (FPR), and two FMLP receptor homologue orphan receptors (FPRH1, FPRH2) to chromosome 19. *Genomics*. 13:437–440.
12. Quehenberger, O., E.R. Prossnitz, S.L. Cavanagh, C.G. Cochrane, and R.D. Ye. 1993. Multiple domains of the *N*-formyl peptide receptor are required for high-affinity ligand binding. Construction and analysis of chimeric *N*-formyl peptide receptors. *J. Biol. Chem*. 268:18167–18175.
13. Durstin, M., J.-L. Gao, H.L. Tiffany, D. McDermott, and P.M. Murphy. 1994. Differential expression of the members of the *N*-formylpeptide receptor gene cluster in human phagocytes. *Biochem. Biophys. Res. Commun*. 201:174–179.
14. Laudanna, C., J.J. Campbell, and E.C. Butcher. 1996. Role of Rho in chemoattractant-activated leukocyte adhesion through integrins. *Science*. 271:981–983.
15. Fiore, S., J.F. Maddox, H.D. Perez, and C.N. Serhan. 1994. Identification of a human cDNA encoding a functional high affinity lipoxin A4 receptor. *J. Exp. Med*. 180:253–260.
16. Su, S.B., W. Gong, J.-L. Gao, W. Shen, P.M. Murphy, J.J. Oppenheim, and J.M. Wang. 1999. A seven-transmembrane, G protein–coupled receptor, FPRL1, mediates the chemotactic activity of serum amyloid A for human phagocytic cells. *J. Exp. Med*. 189:395–402.
17. Su, S.B., J.-L. Gao, W. Gong, N.M. Dunlop, P.M. Murphy, J.J. Oppenheim, and J.M. Wang. 1999. T21/DP107, a synthetic leucine zipper-like domain of the HIV-1 envelope gp41, attracts and activates human phagocytes by using G protein-coupled formyl peptide receptors. *J. Immunol*. 162: 5924–5930.
18. Su, S.B., W. Gong, J.-L. Gao, W. Shen, M.C. Grimm, X.

Deng, P.M. Murphy, J.J. Oppenheim, and J.M. Wang. 1999. T20/DP178, an ectodomain peptide of human immunodeficiency virus type 1 gp41, is an activator of human phagocyte N-formyl peptide receptor. *Blood.* 93:3885–3892.

19. Kilby, J.M., S. Hopkins, T.M. Venetta, B. DiMassimo, G.A. Cloud, J.Y. Lee, L. Alldredge, E. Hunter, D. Lambert, D. Bolognesi, et al. 1998. Potent suppression of HIV-1 replication in humans by T-20, a peptide inhibitor of gp41-mediated virus entry. *Nat. Med.* 4:1302–1307.
20. Gao, J.-L., and P.M. Murphy. 1993. Species and subtype variants of the *N*-formyl peptide chemotactic receptor reveal multiple important functional domains. *J. Biol. Chem.* 268: 25395–25401.
21. Gao, J.-L., E.J. Lee, and P.M. Murphy. 1999. Impaired antibacterial host defense in mice lacking the *N*-formylpeptide receptor. *J. Exp. Med.* 189:657–662.
22. Gao, J.-L., H. Chen, J.D. Filie, C.A. Kozak, and P.M. Murphy. 1998. Differential expansion of the N-formylpeptide receptor gene cluster in human and mouse. *Genomics.* 51:270–276.
23. Takano, T., S. Fiore, J.F. Maddox, H.R. Brady, N.A. Petasis, and C.N. Serhan. 1997. Aspirin-triggered 15-epi-lipoxin A_4 (LXA_4) and LXA_4 stable analogues are potent inhibitors of acute inflammation: evidence for anti-inflammatory receptors. *J. Exp. Med.* 185:1693–1704.
24. Davis, L.G., M.D. Dibner, and J.F. Battey. 1986. Basic Methods in Molecular Biology. Elsevier Science B.V., Amsterdam. 143–146.
25. Ali, H., R.M. Richardson, B. Haribabu, and R. Snyderman. 1999. Chemoattractant receptor cross-desensitization. *J. Biol. Chem.* 274:6027–6030.
26. Foxman, E.F., J.J. Campbell, and E.C. Butcher. 1997. Multistep navigation and the combinatorial control of leukocyte chemotaxis. *J. Cell Biol.* 139:1349–1360.
27. Ahuja, S.K., and P.M. Murphy. 1996. The CXC chemokines growth-related oncogene (GRO)α, GROβ, GROγ, neutrophil-activating peptide-2 and epithelial cell-derived neutrophil-activating peptide-78 (ENA-78) are potent agonists for the type B, but not the type A, human interleukin-8 receptor. *J. Biol. Chem.* 271:20545–20550.
28. Neote, K., D. DiGregorio, J.Y. Mak, R. Horuk, and T.J. Schall. 1993. Molecular cloning, functional expression, and signaling characteristics of a C-C chemokine receptor. *Cell.* 72:415–425.
29. Ludwig, A., F. Petersen, S. Zahn, O. Gotze, J.M. Schroder, H.D. Flad, and E. Brandt. 1997. The CXC-chemokine neutrophil-activating peptide-2 induces two distinct optima of neutrophil chemotaxis by differential interaction with interleukin-8 receptors CXCR-1 and CXCR-2. *Blood.* 90:4588–4597.